Al-Mustansiriyah Journal of Science
ISSN: 1814-635X (print), ISSN:2521-3520 (online)
Volume 29, Issue 1, 2018
DOI:http://doi.org/10.23851/mjs.v29i1.278

Research Article **Open Access**

FTIR and Optical Properties of NiO Doped Cr_2O_3 Nanoparticles Synthesis by Hydrothermal Method

Tunis B. Hassan[1*], Ghuson H. Mohammed[2]
Ministry of Education, Directorate General for Vocational Education, IRAQ
Department of Physics, College of Science, University of Baghdad,IRAQ
*Correspondent email: Tunis20151@yahoo.com

ArticleInfo

Received
15\Oct.\2017

Accepted
25\Dec.\2017

Abstract
Pure and Nickel oxide doped chromium (III) oxide (Cr_2O_3) nanoparticals are synthesized by hydrothermal technique. The effect of dopant Ni concentration on the structural behavior of Cr_2O_3 nanoparticles was examined by X-ray diffraction. The average crystallite size of the synthesized nanoparticles was measured from XRD patterns using Scherrer equation and was decreased from 22nm to 12.9 nm with the increasing Nio concentration in Cr_2O_3 from (0, 0.01, 0.06, and 0.10). Morphologies and compositional elements of the synthesized nanoparticles were observed by the field emission scanning electron microscopy (FESEM) and energy dispersive X-ray (EDX) spectroscopy, respectively. The optical property of the samples was measured by ultraviolet - visible (UV-Vis.) absorption spectroscopy. The observed optical band gap value ranges from 2.3eV to 2.5eV for Ni doped nanoparticles.

Keywords: Cr_2O_3 Nanoparticles, Hydrothermal Method, Structural Properties, Optical Properties.

الخلاصة
تم تحضر اوكسيد الكروم النانوي النقي والمطعم بنيكل اوكسيد بالطريقة الهيدروحرارية المائية. تم دراسة تأثير التطعيم لتركيز اوكسيد النيكل على سلوك التركيب لجسيمات اوكسيد الكروم النانوي بواسطة حيود الأشعة السينية. تم قياس معدل الحجم البلوري للجسيمات النانوية المحضرة بواسطة حيود الاشعة السيتية باستخدام معادلة شرر وكان ينخفض من 22nm إلى 12.9 نانومتر مع زيادة تركيز اوكسيد النيكل في اوكسيد الكروم من (0، 0.01، 0.06، 0.10). وقد لوحظت مورفولوجيه والعناصر التركيبية للجسيمات النانوية المحضرة من قبل المجهر الإلكتروني المسح الضوئي الانبعاثات وطاقة التشتت الأشعة السينية التحليل الطيفي، على التوالي. تم قياس الخصائصالبصرية للعينات بواسطة الأشعة فوق البنفسجية المرئية وتتراوح قيمة فجوة البصرية من 2.3 الكترون فولت إلى 2.5الكترون فولت لجسيمات اوكسيد النيكل المطعمة.

Introduction

Metal oxides play a very important role in many areas of chemistry, physics and materials science. The metal elements are able to form a large diversity of oxide compounds [1]. These can adopt a vast number of structural geometries with an electronic structure that can exhibit metallic, semiconductor or insulator character. In technological applications, oxides are used in the fabrication of microelectronic circuits, sensors, piezoelectric devices, fuel cells, coatings for the passivation of surfaces against corrosion, and as catalysts [2]. The application of nanomaterials utilizes not only chemical composition but also the size, shape and surface dependent properties [3]. Nanoparticles can be noncyrstalline, polycrystalline or single crystalline and can be produced with a variety of methods [4]. Semiconducting nanostructures represent one of the most important frontiers in advanced material research due to their peculiar optical, electrical, thermoelectric properties and potential applications in nanodevices. Semiconducting oxides are the fundamentals of smart devices as both the structure and morphology of these materials can be controlled precisely and accordingly, are referred as functional oxides [5][6]. Nanoparticles often have novel chemical and physical properties. Such as, the optical, chemical and electronic proper-

ties of nanoparticles may be largerly different from those of each material in the bulk [7]. Chromium sesquioxide, (Cr_2O_3), is an anti-ferromagnetic [8] is one of the most important wide band gap (Eg≈3eV) p-type semiconductor [9] transition metal-oxide material [10]. This kind of p-type is a wide band gap oxide semiconductor. Many crystalline modifications of chromium oxides: such as rutile (CrO_2), CrO_3, CrO_4, corundum (Cr_2O_3), Cr_2O_5, and Cr_5O_{12} has been reported. Among these modifications, Cr_2O_3 is the most stable magnetic-dielectric oxide-material [11].

In this paper, we report synthesis of pure Cr_2O_3 and Ni doped Cr_2O_3 nanoparticles by hydrothermal method and its characterization by means of X-ray diffraction (XRD), Filed Emission scanning electron microscope (FESEM), UV- Vis and FTIR spectroscopic methods which will give much valuable information about these materials.

Materials and Methodology

A. Cr_2O_3 nanoparticles were synthesized by modified hydrothermal method.

For the synthesis of undoped Cr_2O_3 nanoparticl, Chromic nitrate, [$Cr(NO_3)_3.9H_2O$], sodium hydroxide (NaOH) and poly vinyl alcohol (PVA) were used.0.1M [$Cr(NO_3)_3.9H_2O$] was added into 25ml of ethanol absolute was stirred for 1h at room temperature to form a homogeneous solution.

3.0 g of PVA were dissolved in 50 ml deionized water and stirred for 30 min. Simultaneously, a 10ml NaOH (10M) was added drop wise into this aqueous $Cr(NO_3)_3.9H_2O$. During the addition of NaOH into aqueous solution, the solution was heated at 80 ^oC [12]. At last, the final solution was transferred into a 100 ml Teflon-lined stainless steel autoclave. The autoclave was sealed and maintained at 150 ^oC for 24 h, and then allowed to cool to room temperature naturally. After terminating the reaction in desired time, the resulted solid projects, washed with distilled water and ethanol to remove the ions possibly remaining in the final product, and dried in air at 60 ^oC for 4 h. Finally, the prepared powder will be undergone to calcination process for 2 hour at 400 ^oC. NiO doped Cr_2O_3 nanoparticles were prepared.

Where the molar concentration was the same for each [(0.1), Cr $(NO_3)_3.9H_2O$ and $(NO_3)_2.6H_2O$] of the percentages used represented a value (NiO=0.01, 0.06, 0.10).

B.Preparation of Thick Films

The films were prepared using hydrometallic technique for each nanopartical and nanocomposite .The thixotropic paste was formulated by mixing the fine powder of as prepared with the solution of (a temporary binder) in a mixture of organic solvents such as ethyl acetate. The ratio of inorganic part to organic part was kept at 70:30 in formulating the paste. This thixotropic paste was used to deposit thick films on ultrasonically cleaned silicon substrate (2cm x 1cm) using [13]. The films were fired at 550^oC for 30 min.

Characterization

Recently nanostructured semiconducting materials are synthesized by different physical and chemical methods. This represents the various characterization techniques utilized in the present work and it also includes the basic principles of the characterization techniques in X-ray Diffraction (XRD) 40 kV and 30 mA with monochromatic CuKα radiation (λ=1.54056 Å) and the scanning 2θ range from 20 to 70º., Atomic Force Microscopy (AFM), field emission scanning electron microscopy **(**FE-SEM), Energy dispersive X-ray analysis (EDX) was used to estimate the composition of the materials. Fourier transform infrared (FTIR) by TENSOR 27 range of 400-4000 cm^{-1}.The optical absorbance spectrum in the wavelength range (200-1100) nm was recorded at room temperature using 2601.

Results and Discussion

Figure1 displays X-ray diffraction patterns of the as-prepared Cr_2O_3 and NiO-doped Cr_2O_3 films on glass substrate by screen print at dried 550^oC for 30mint. The XRD spectra of NiO doped Cr_2O_3consist of (012) (104), (110), (113), (202), (024), and (116) peaks, and all the observed diffraction peaks can be indexed to Cr_2O_3 rhombohedral structure. No diffraction peaks of other structures were detected in these samples, indicating that the Ni ion successfully occupied Cr_2O_3 lattice site and there were no secondary phases or precipitates in the samples.

The intensities of the diffraction peak in pattern Figure. 1(b) were higher than those of the peak in patterns Fig. 1(c-f), indicating that the addition of Cu dopant as well as the increasing concentration of dopant in Cr_2O_3 matrix slightly decreases the crystalline of the samples. The addition of dopant not only decreases the diffraction peak intensity of the XRD spectra, the broadening of the dominant peaks also slightly increased. The crystallites sizes of the Cr_2O_3 and NiO doped Cr_2O_3 are estimated using Debye–Scherrer equation [14]:

$$D \frac{K\lambda}{\beta.cos\theta} \quad \ldots\ldots\ldots\ldots\ldots\ldots\ldots\ldots\ldots\ldots (1)$$

where D is the crystallite size, λ is wavelength of radiation used, β is the full width at the half maximum peak at diffraction angle 2θ.

The average values of grain sizes are 22 nm, 19.4 nm, 18.3nm and 12.9nm for the Cr_2O_3, $(Cr_{0.99}Ni_{0.01})$ O_4, $(Cr_{0.94}Ni_{0.06})$ O_4, and $(Cr_{0.90}Ni_{0.10})$ O_4 respectively, Also the crystallite size decreases with increasing concentration of Ni from (0.0 to 0.10) in Cr_2O_3 lattices.

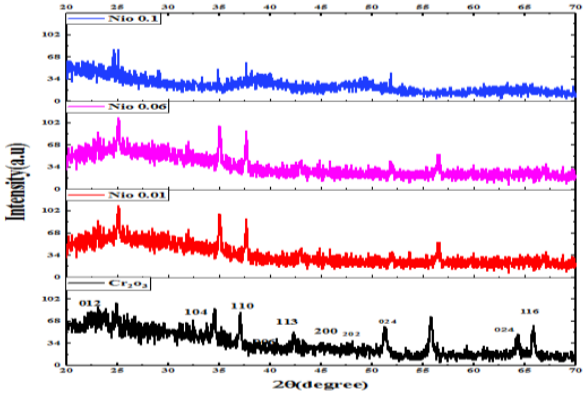

Figure1: ThinFilms x-ray diffraction pattern of (A) Cr_2O_3 nanoparticles (B) 0.01(C) 0.06(D) 0.10.

This could be ascribed to the difference between the radii of Ni^{2+} and Cr^{3+}. The radius of Ni^{2+} was 0.69 A°, which was larger than that of Cr^{3+} (0.62 A°) at the same. Therefore, the substitution of Ni^{2+} by Cr^{3+} induced the high angle shift of diffraction peaks, confirming that Ni^{2+} is incorporated into the Cr^{3+} lattice. Although doping does not alter the crystal structure, it causes the lattice constant to change as evidence of the (101) peak position shift. Although the change is very little, the concentration of dopant plays a role in the c-axis constant [15].The AFM image in two and three dimension view of undoped Cr_2O_3 nanoparticals, and NiO(0.01,0.06,and 0.10) doped Cr_2O_3 NPs are shown in Figures2(A,B,C,D) respectively. The results of AFM doped dimameter of the particles were average of 45-60 nm. The grain size and roughness average decreased with increase concentration of NiO thin film as shown in Table 1.

Table 1: The Average Particles sizes, Roughness average for un-doped and doped Cr_2O_3 nanoparticals with NiO.

Sample	Particle size (nm)AFM	Particle size (nm)XRD	Roughness average (nm)
Cr_2O_3	60	22	0.404
0.01	55	19.4	0.443
0.06	51	18.3	0.338
0.10	46	12.9	0.546

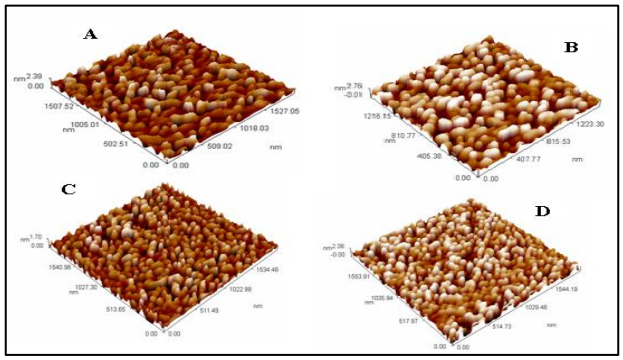

Figure 2: AFM particale size distribution of Cr_2O_3NPs and NiO (0.01, 0.06, and 0.10).

The FESEM micrographs of undoped Cr_2O_3 nanoparticals and doped with NiO (0.01, 0.06, and 0.10) films were fired at 550°C for 30 min are shown in Figure3 respectively. FESEM analysis provides the information about the shape and size. The results of FESEM showed that the average diameter 30-50nm. It can also be seen that the shape of synthesized Cr_2O_3 nanoparticals were homogenous, spherical. The EDAX analysis was carried out and the results are represented in. Figure 4 shows the EDS

spectra of the synthesized Cr_2O_3 nanoparticles. The surface of the Cr_2O_3 and NiO doped nanoparticles also exhibited elements of O, Cr and Ni. Here the Nickel is present in elemental form. These results are consistent with the XRD data.

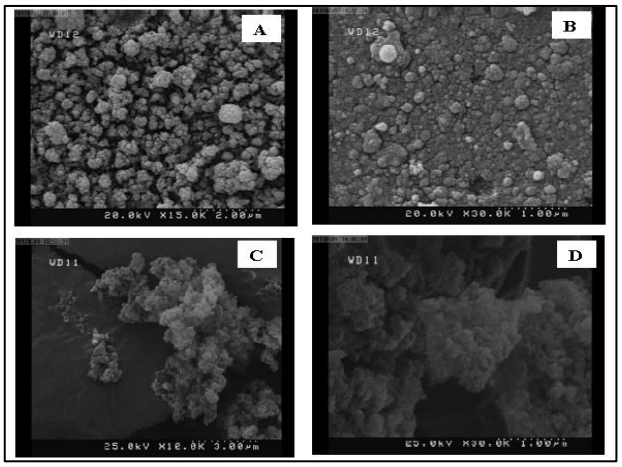

Figure 3: FESEM image Figure of Cr_2O_3NPs and NiO (0.01, 0.06, and 0.10).

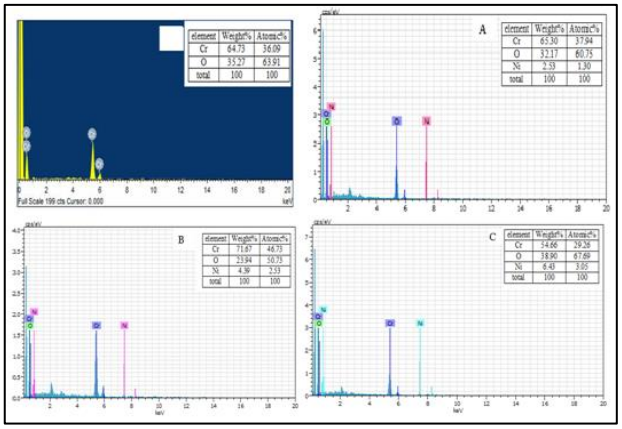

Figure 4: EDX analysis of Cr_2O_3NPs (A) 0.01(B) 0.06 (C) 0.10.

The FTIR spectra obtained from Cr_2O_3 nanoparticals prepared by the hydrothermal are shown in Figures (5A-D).The spectra of Cr_2O_3 NPs are shown in Figure. A broad band at 3420 cm^{-1} corresponds to the stretching modes of surface OH groups. Metal oxide Cr_2O_3 generally reveal absorption bands below 1000 cm^{-1} due to inter-atomic vibrations. Two sharp peaks displayed at 652 and 562 cm^{-1} attributed to Cr-O stretching modes, are clear evidence for the presence of the crystalline Cr_2O_3 [16].

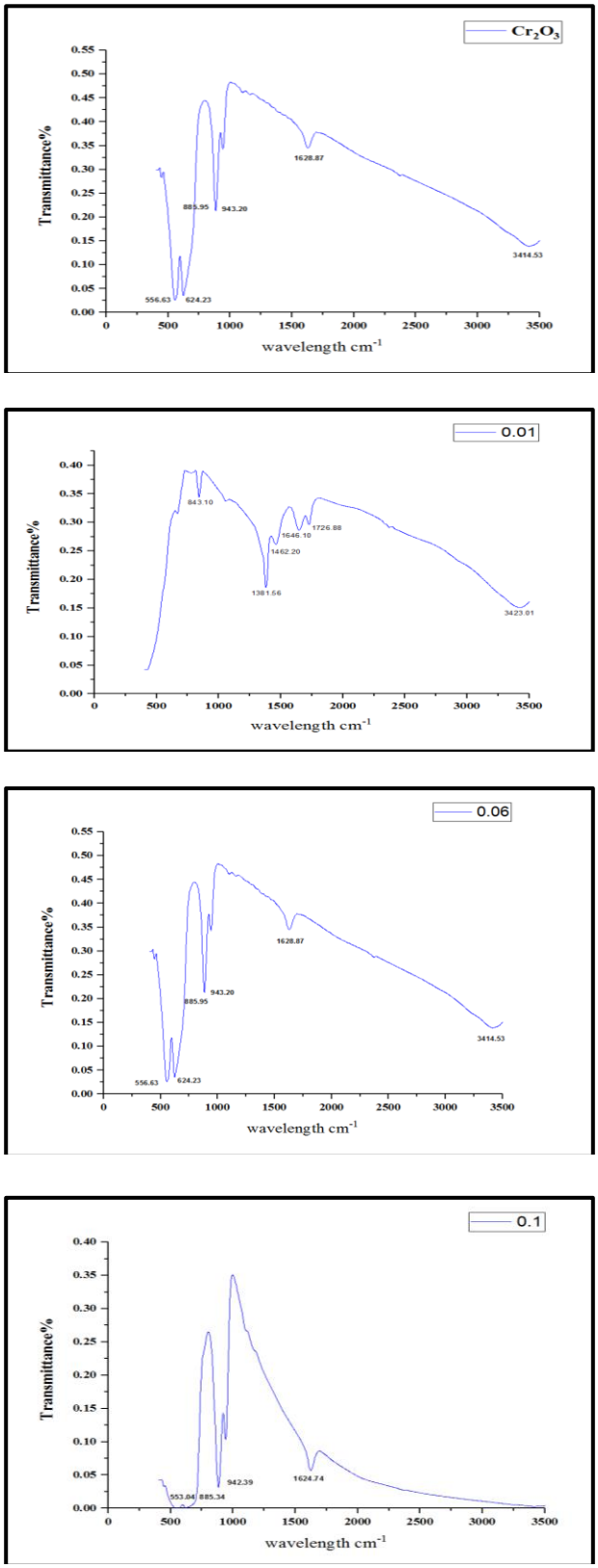

Figure 5: The FT-IR for undoped and doped (A) Cr_2O_3 NPs (B) 0.01(C) 0.06 (D) 0.10.

Interestingly, it was observed that intensity of the higher frequency decrease with increase in NiO doped concentration. This mode is attributed to the vibrations of Cr–O–Ni local

bonds and modes from defect states which accompanies the enhanced NiO doping in Cr_2O_3. The optical properties of synthesized nanomaterials were determined by absorption spectra obtained from UV-visible spectroscopy. The band gap of synthesized nanoparticles was based on the nature of the electronic transition and was determined by the variation of optical coefficient with wavelength. The relationship between absorption spectra and the energy gap was described by Tauc's expression mentioned in the equation [17]:

$$(\alpha h\upsilon) = A (h\upsilon - E_g)^n \quad \ldots\ldots\ldots\ldots\ldots\ldots (2)$$

where, α is the absorption coefficient, A is a constant, E_g is the bandgap energy of the material and exponent n = ½ for direct transition. Figure 6 shows the optical absorption spectrum of the pure, NiO (0.01, 0.06, and 0.10) doped Cr_2O_3 nanoparticles. The observed optical bandgap energy values2.54 are and 2.60, 2.65, and 2.75, eV for Pure Cr_2O_3, (0.01, 0.06, and 0.10) NiO doped Cr_2O_3 nano particles respectively. The bandgap observed for the doped Cr_2O_3 nanocrystals are higher than the pure Cr_2O_3 .It is known that semiconductor nanocrystals with crystallite size significantly smaller than the exciton Bohr radius show size-dependent optical properties due to the strong quantum confinement effect for the charge carriers. A weak quantum confinement effect occurs when the crystallite size is larger than the Bohr radiu. It is known that the typical exciton Bohr radius for Cr_2O_3 is 3nm [18]. The increase of E_g may be due to reduction in crystallite sizes with comparable radius to that of Cr^{3+} ions. In order to picture implicit, the variation of E_g and crystallite size with respect to various concentrations of Cu in Cr_2O_3 system.

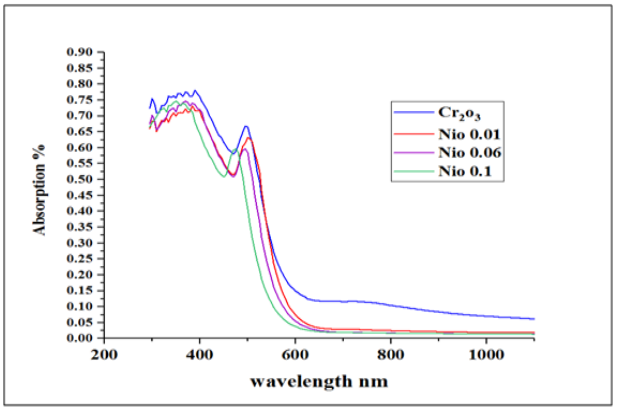

Figure 6: The absorption for undoped and doped (A) Cr_2O_3NPs (B) 0.01 (C) 0.06 (D) 0.10.

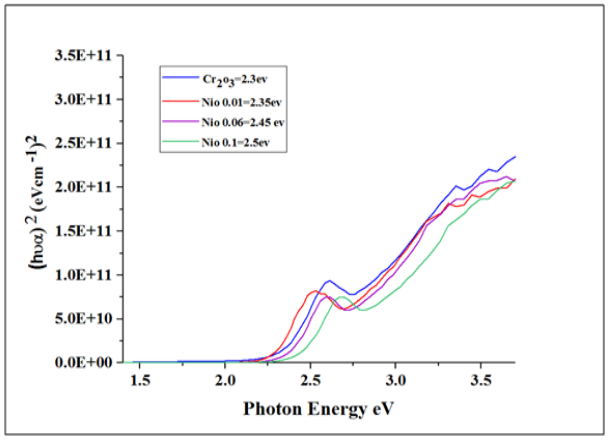

Figure 7: The energy gap for undoped and doped (A) Cr_2O_3 NPs (B) 0.01 (C) 0.06 (D) 0.10.

Conclusions

In this paper, we have described the synthesis, structural, morphological and optical characterization of a series of NiO doped Cr_2O_3 nanoparticles by hydrothermal technique. Nickel doped Cr_2O_3 nano particles different concentrations. Regarding the structural properties, a systematic decrease in the unit cell volume, crystallite size, and changes in the FWHM parameter were observed in concurrence with the presence of NiO dopant in the prepared nanoparticles. The best results were obtained. The structure and phase of the as prepared materials were determined by using the XRD, AFM, and FESEM. The average size of the particles was measured by the Scherer formula for both doped and pure Cr_2O_3. The morphology and structural analysis was done by the SEM. Further the presence of NiO dopants was confirmed EDAX. And prepared nanoparticles

were also analyzed for FTIR, UV-Visible spectroscopic techniques. The optical band values (E_g) values were further obtained from Tauc plots.

Reference

[1] Rodríguez, José A., and Fernández-García, Marcos, " Synthesis, Properties, and Applications of Oxide Nanomaterials", JohnWiley & Sons, Inc., USA, 2007.

[2] Fernández-Garcia, Marcos and Rodriguez, José A., 2007, "Metal Oxide Nanoparticles", Brookhaven National Laboratory, USA, 2007.

[3] T. Pradeep, "Nano: The Essentials, understanding Nanoscience and nanotechnology", Tata Mc-Graw-Hill Publishing company Limited, New Delhi 2007.

[4] Bihari B., Eilers, H., Tissue, B. M. "Spectra and dynamics of monoclinic Eu2O3 and Eu3+:Y2O3nanocrystals", Journal of Luminescence,1997.

[5] Kalele1, Suchita, Gosavi, S. W., Urban, J. and Kulkarni,S. K., "Nanoshell particles: synthesis", properties and applications, Current Science, vol. 91, no. 8, pp.1038- 1052, 2006.

[6] Chen, Yongfen, Johnson, Eric, and Peng, Xiaogang, " Formation of Monodisperse and Shape-Controlled MnO Nanocrystals in Non-Injection Synthesis: Self-Focusing via Ripening ", American Chemical Society, 129, pp.10937-10947, 2007.

[7] Gleiter, H., Weissmuller, J., Wollersheim, O., and Wurschum, R., " Nanocrystalline Materials: A way to Solids with Tunable Electronic Stractures and Properties ", Acta mater. 49, pp. 737–745, 2001.

[8] Tabbal, M., Kahwaji, S., Christidis, T.C., Nsouli, B., and Zahraman, K., " Pulsed laser deposition of nanostructured dichromium trioxide thin films, Thin Solid Films 515 ", pp. 1976–1984, 2006.

[9] Cao, Huaqiang, Qiu, Xianqing, Liang, Yu, Zhao, Meijuan and Zhu, Qiming, " Sol-gel synthesis and photoluminescence of p-type semiconductor Cr2O3 nanowires ", Appl. Phys. Lett. 88, pp. 241112-1-4, 2006.

[10] Aghaie-Khafri, M., Kakaei Lafdani, M.H., " Anovel method to synthesize Cr2O3 nanopowders using EDTA as a chelating agent, Powder Technology 222" , pp. 152–159, 2012.

[11] Ivanova, T., Gesheva, K., Cziraki, A., Szekeres, A., and Vlaikova, E., " Structural transformations and their relation to the optoelectronic properties of chromium oxide thin films" , Journal of Physics: Conference Series 113, pp.1-6, 2008.

[12] Jain, G. H., " Synthesis of Ni-doped ZnO Nanorods by Hydrothermal Route and Its Gas Sensing Properties ", Sixth International Conference on Sensing Technology (ICST), vol. 7, no. 2 pp.831-835, 2012.

[13] Anjum, Safia, " Growth of Nano-Structured Thin Films of Magnetic Materials by PLD Technique", A Dissertation as partial of the requirements of Doctor of Philosophy in Physics, Faculty of Natural Sciences, University of Engineering and Technology, 2010.

[14] Taylor, Nick," Energy Dispersive Spectroscopy ", John Wiley & Sons Ltd, The Atrium, Southern Gate, Chic ester, West Sussex, 2015.

[15] Yamazoe, Noboru, Sakai, Go and Shimanoe, Kengo," Oxide semiconductor gas sensors " , Catalysis Surveys from Asia Vol. 7, No. 1, pp.63-75, 2003.

[16] Bhuiyan, M.R.A., and Rahman, M.K., " Synthesis and Characterization of Ni Doped ZnO Nanoparticles" , I.J. Engineering and Manufacturing, No.1, pp.10-17, 2014.

[17] Al-Kuhaili, M.F., and Durrani, S.M.A., " Optical properties of chromium oxide thin films deposited by electron-beam evaporation ", Optical Materials 29, pp. 709–713, 2007.

[18] Mohanapandian, K., and Krishnan, A., " Effect of Concentration of Ni2+ on the Physio Chemical Properties of Cr2o3 Nano Particles", Adv. Studies Theor. Phys., Vol. 8, No. 6, pp. 267 – 276, 2014.